

Investigation on the Interpenetrating Polymer Networks (IPNs) of Polyvinyl Alcohol and Poly(*N*-vinyl pyrrolidone) Hydrogel and Its *In Vitro* Bioassessment

Mei Gong,¹ Li Zhang,¹ Yi Zuo,¹ Qin Zou,¹ Yanying Wang,² Li Wang,¹ Yubao Li¹

¹Research Center for Nano-Biomaterials, Analytical and Testing Center, Sichuan University, Chengdu 610064, China

²Inorganic Chemistry, College of Chemistry, Sichuan University, Chengdu 610064, China

Received 25 February 2011; accepted 24 September 2011

DOI 10.1002/app.36247

Published online 31 January 2012 in Wiley Online Library (wileyonlinelibrary.com).

ABSTRACT: Poly(vinyl alcohol) (PVA) and poly(*N*-vinyl pyrrolidone) (PVP) composite hydrogel with interpenetrating polymer networks (IPNs) was prepared by *in situ* polymerization and compared with pure PVA hydrogel. The prepared IPN hydrogel was characterized by infrared spectroscopy (IR), differential scanning calorimetry (DSC), dynamic mechanical analysis (DMA), X-ray photoelectron spectroscopy (XPS), and scanning electron microscopy. The mechanical property and cell culture were also tested. The results show that PVP can chemically bond with PVA and form uniform blend hydrogel. The content of PVP can affect the structure, crystallinity, glass transition temperature (T_g), and mechanical property of the hydrogel. The T_g of the PVA hydrogel is 2.7°C while the T_g of the IPN hydrogel is -37°C. The IPN hydrogel has lower glass tran-

sition temperature, corresponding to better elastic properties, and has better mechanical performance on stretch and compression than PVA hydrogel. The crystallinity (X_c) of PVA hydrogel and IPN hydrogel is 65.3 and 26.3%, respectively. The DMA curves and XPS analysis suggest that PVA and PVP are well miscible on a molecular level in the IPN hydrogel. The cell proliferation trend demonstrates that the addition of PVP has a positive influence on the cell growth and the IPN hydrogel may be used as a promising biomaterial for artificial cartilage substitute. © 2012 Wiley Periodicals, Inc. *J Appl Polym Sci* 125: 2799–2806, 2012

Key words: interpenetrating polymer network; *in situ* synthesis; poly(vinyl alcohol); poly(*N*-vinyl pyrrolidone); hydrogel; cytocompatibility

INTRODUCTION

Poly(vinyl alcohol) (PVA) hydrogel used as a biomaterial has been studied extensively and its excellent biocompatibility and physical properties have been confirmed.¹ In virtue of high water content and viscoelastic characteristics similar to human cartilage and soft tissue, PVA hydrogels have been applied as functional materials in clinical application for dialysis membranes, wound dressing, artificial skin, cardiovascular devices, drug delivery, and spine disc replacement.² Recently, PVA hydrogel has been highlighted in replacing diseased articular cartilage due to its excellent biotribological properties.³ However, the major problem of PVA hydrogel for artificial cartilage is that it has not enough stiffness as natural cartilage.⁴ As a prosthetic implant, a stabilized structure of hydrogel is required within physiological environment.

In previous study, 1% poly(*N*-vinyl pyrrolidone) (PVP) has been blended into PVA to stabilize the hydrogel for replacement of the degenerated nucleus pulposus.⁵ PVA/PVP blend films were found to provide a great stabilization effect on the thermal decomposition of *S*-nitrosoglutathione during tumor therapeutic process.⁶ We also prepared a mixture of PVA and PVP,⁷ however, these PVA/PVP hydrogels were produced by direct blending, only simple and physical network forms internally. It is known that the amount and type of crosslinks will influence many of the hydrogel properties. Thus, uniformly crosslinked networks need to be synthesized for hydrogel application.

Chemical reagent allows facile crosslinking of hydrogels; however, the residual chemical crosslinker is usually toxic for biological application.⁸ Recently, interpenetrating polymer networks (IPNs) as a functional structure efficiently improve the physicochemical properties of hydrogels. Many researchers have reported pH- and temperature-responsive or electrically responsive IPN hydrogels composed of PVA and other polymers like poly(acrylic acid), poly(vinyl-pyrrolidone), and polyallylamine/chitosan.⁹ IPN hydrogel is a combination of two or more polymers simultaneously gelatinizing. They can also be described as polymer gels held

Correspondence to: Y. Li (nic7504@scu.edu.cn) or Y. Zuo (zoe@vip.sina.com).

Contract grant sponsor: China 973 Project; contract grant number: 2007CB936102.

together by permanent entanglement.¹⁰ It is reasonable to expect significant changes in chemical and physical properties when two individual polymers are blended together with hydrogen bonding, ionization and dipolarization, or π -electrons hybridization.^{11,12} As a corollary, IPNs can provide stable properties for hydrogels.

In this study, IPNs of PVA and PVP were fabricated by *in situ* polymerization. Viscoelastic behavior and thermal characteristics were tested and calculated, using dynamic mechanical analysis (DMA) and differential scanning calorimetry (DSC). The physical and chemical properties were discussed to verify the formation of IPNs structure. The morphology, mechanical properties, and cytocompatibility were also evaluated.

EXPERIMENTAL

Materials

Poly(vinyl alcohol) with a mean degree of polymerization 1700 ± 50 , hydrolysis degree 99%, residual content of acetate groups 0.13%, and content of PVA more than 90.5 wt % was obtained from Chengdu Chemical Agent (China). The contents of carbon and hydrogen of PVA determined by Element Analyzer (Carlo Erba 1106, Italy) were 52.20 ± 0.36 and 9.75 ± 0.12 wt %, respectively. *N*-vinyl pyrrolidone was purchased from the Aladdin (China). Dimethylsulfoxide (DMSO, A.R.) was supplied by Chengdu Chemical Agent (China). All other chemicals used were analytical grade.

Sample preparation

PVA (30 g) was dissolved into 80% DMSO (170 g) aqueous solution at 90°C for 3 h to form the 15% PVA solution. *N*-vinyl pyrrolidone was poured into PVA solution at 50°C with stirring to obtain the mixture solution. To form the mixture solution, 30 wt % hydrogen peroxide and 25 wt % ammonia were added as initiators for free radical polymerization. The reaction was lasted for 1–2 h in N_2 atmosphere until the temperature of mixed solution decreased. Then the temperature was risen to 70°C and *N,N*-methylene-*bis*-acrylamide (2 g) was added with slow stirring to form crosslinked PVP (PVPP) and thus obtained the blend slurry (PVA/PVP = 300 wt %). The slurry was cast into mould and subjected to one freeze-thawing cycle by keeping at -28°C for 8 h and at room temperature for 4 h. The freeze-thawing cycle was repeated for seven times to form crosslinked PVA. Thereafter, the IPN hydrogel was immersed into deionized water to remove DMSO. A schematic synthesis diagram of the PVA/PVP IPN hydrogel was shown in Figure 1.

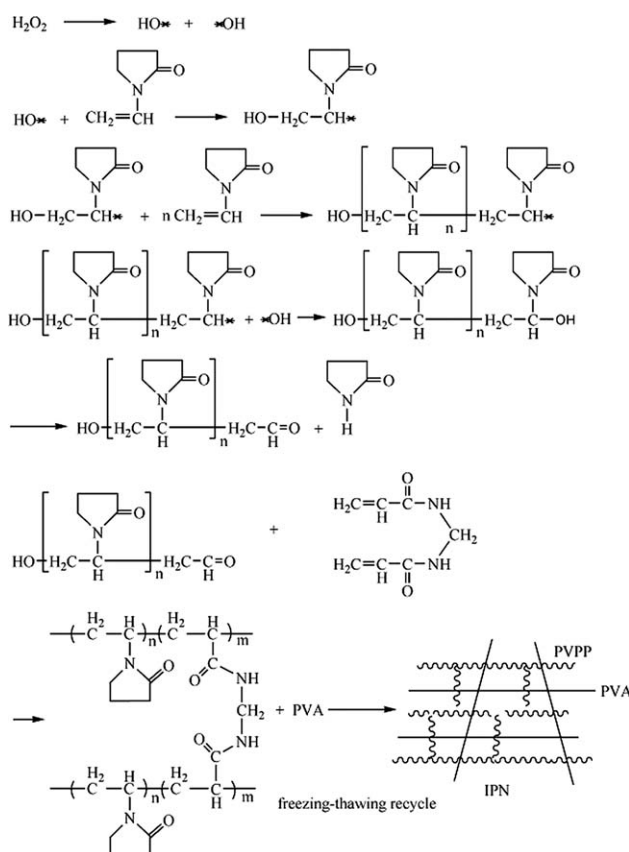


Figure 1 Schematic synthesis diagram of PVA/PVP IPN hydrogel.

Tests

The DMA of the hydrogel blend was carried out by means of a DMA 242 (NETZSCH Instruments, Germany) at a frequency of 1.66 Hz from -90 to 120°C . Samples with dimension of $1.00 \times 0.26 \times 0.12$ cm^3 were submitted to sinusoidal deformation with 0.20 mm of amplitude. The samples were heated in steps of 2°C , remaining at each temperature for enough time to reach thermal equilibrium.

DSC was conducted on a DSC instrument (204 F1, Netzsch, Germany). In aluminum pan, 5–10 mg of a dried sample was placed. A nitrogen purge through the sample chamber was implemented to obtain a uniform, stable thermal environment. The samples, in aluminum pans, were initially cooled to -20°C and then heated until 250°C at $10^\circ\text{C}/\text{min}$ to erase their previous thermal history. The samples were subsequently cooled to 40°C at $10^\circ\text{C}/\text{min}$ and submitted to a second heating at $10^\circ\text{C}/\text{min}$ until 250°C . Only the thermograms corresponding to the second heating scan were used in the analysis.

Infrared (IR) spectra of samples were recorded with a FTIR spectrophotometer (PerkinElmer). Film samples were scanned from 500 to 4000 cm^{-1} .

X-ray photoelectron spectroscopy (XPS) analysis was carried out on a Kratos, XSAM800 spectrometer

(UK) employing Al K α (1486.6 eV) excitation radiation. The charging shift was referred to the C1s line emitted from the saturated hydrocarbon at 285.0 eV. The surface elemental composition was calculated from the peak area with a correction for atomic sensitivity.

Scanning electron micrograph

The micrographs of the dried IPN hydrogels were recorded on a scanning electron microscopy (SEM, Hitachi S-4800LV, Japan). All the specimens were sputtering coated with gold prior to observation.

Cylindrical hydrogel specimens ($\Phi 12 \times 4$ mm²) were used for compressive strength test by a universal testing machine (Instron model 4400, UK) at room temperature and at a probe speed of 0.5 mm/min until the specimen reached 60% relative deformation. The corresponding value was used as the compressive strength. The mechanical properties such as tensile strength and elongation at break were also tested by Shimadzu AG-IC 50KN-universal test machine, Japan. The wet samples were used for the mechanical characterization.

Bone marrow was collected from the femora of young adult male Wistar rat. The marrow-derived mesenchymal stem cells (MSCs) were cultured in flasks at 37.8°C and 100% humidity with 5% CO₂ in Dulbecco's Modified Eagle Medium (DMEM, Gibco). The medium was supplemented with 10% volume fraction of fetal bovine serum (Gibco), 50 mg mL⁻¹ gentamicin (Gibco), 0.3 mg mL⁻¹ fungizone (Gibco), 5 mg L⁻¹ L-ascorbic acid (Gibco), 2.16 g L⁻¹ b-glycero-phosphate (Sigma), and 10M dexamethasone (Sigma). The MSCs at passage III were removed into the culture medium. The medium was changed every 2 days.

The MSCs were cultured and cocultured with hydrogel samples (2×10^4 cells/cm²) according to the given method.¹³ Each specimen ($\Phi 8.0 \times 1.0$ mm²) was sterilized by ethylene oxide gas, immersed in a well with 2 mL of fresh medium (without cells), and extracted overnight in an incubator. The MSCs cultured in medium for 3 days were seeded on the top of prewetted specimens. The specimens were then placed in the wells of plastic dishes (24-well cell culture plates, Corning) and left undisturbed in an incubator for 3 h to allow the cells to attach, and additional 1 mL culture medium was added into each well. The cell/hydrogel constructs were cultured in a humidified incubator at 37°C with 95% air and 5% CO₂ for 1, 4, 7, and 11 day(s). The medium was changed every 2 days.

Cell proliferation was measured at 1, 4, 7, and 11 day(s) using MTT assay. MTT reagent (3-[4,5-dimethylthiazole-2-yl]-2,5-diphenyltetrazolium bromide) was enzymatically converted by living cells into a

blue/purple formazan product. The intensity of the colored formazan was directly related to the number of viable cells and thus to their proliferation *in vitro*. MTT reagent was added to each specimen in well and incubated at 37°C for 4 h. The colored formazan product was solubilized into solution with dimethyl sulfoxide (DMSO) and the solution of each specimen was removed out for assay. Absorbance was read on a microplate reader (test wavelength: 490 nm).¹⁴ The result was expressed in absorbance as a relative cell activity on the hydrogel specimens compared with that in control (plastic).

Fluorescent chemical detection of 1'-dioctadecyl-3,3',3'-tetramethylindocarbocyanineperchlorate (DiI) was performed on the attached MSCs at passage III in culture. The morphology of MSCs cultured with IPN hydrogel specimens at day 3 and 7 was observed by fluorescence microscopy (Nikon TE300, Japan). For further visualization of the growth and distribution of MSCs on the surface of each specimen, MSCs were pre-labeled with fluorescent DiI (Molecular Probes) at 37°C for 20 min following the manufacturer's protocol. The labeled cells were then seeded on discs as described in the previous section. The cells grown on the discs were then observed by a fluorescence microscope (Nikon TE300, Japan) at day 3 and 7 after seeding.

Quantitative data were presented as means \pm standard deviation (SD). Statistical analysis was assessed by t-test and one-way analysis of variance (ANOVA) using SPSS 13.0. A value of $P < 0.05$ was considered statistically significant.

RESULTS AND DISCUSSION

Dynamic mechanical analysis

The DMA experimental result reveals a difference in dynamic mechanical behavior for the PVA and IPN hydrogel samples. The storage modulus E' represents the stiffness of a viscoelastic material and is proportional to the energy stored during a loading cycle. It is roughly equal to the elastic modulus for a single, rapid stress at low load, and reversible deformation. The storage modulus in Figure 2 shows that the glass transition temperature (T_g) of IPN hydrogel shifts distinctly to lower temperature. The glass transition temperature is a unique value for material that shows a start point from a glass phase to a rubber phase and is a start point of the molecular movement.

The loss modulus E'' is defined to be proportional to the energy dissipated during one loading cycle. It represents energy lost as heat and is a measure of vibrational energy that has been converted during vibration and that cannot be recovered. The real part of the modulus can be used for assessing the elastic

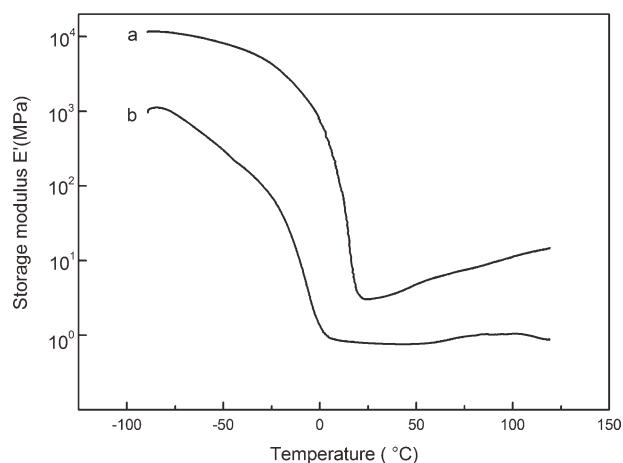


Figure 2 Storage modulus for PVA hydrogel (a) and IPN hydrogel (b) samples.

properties and the imaginary part for the viscous properties. From Figure 3, the curves also show that IPN hydrogel has lower glass transition temperature, corresponding to better elastic properties.

The loss factor $\tan \delta$ is the ratio of loss modulus to storage modulus and is expressed as a dimensionless number. A high $\tan \delta$ value is indicative of a material that has a high, nonelastic strain component, while a low value indicates one that is more elastic. In Figure 4, the $\tan \delta$ curve generally shows the movement of a small group in polymer chains and the interfacial characteristics between PVA and PVP, both hydrogel samples have a certain level of viscoelasticity. The T_g of the PVA hydrogel is 2.7°C while the T_g of the IPN hydrogel is -37°C . Glass transition temperature is an important indicator to study the miscible degree of two mixing polymers. The DMA curves show that the IPN hydrogel is miscible on a molecular level. Since the T_g shifts to lower temperature after blending, the transition is

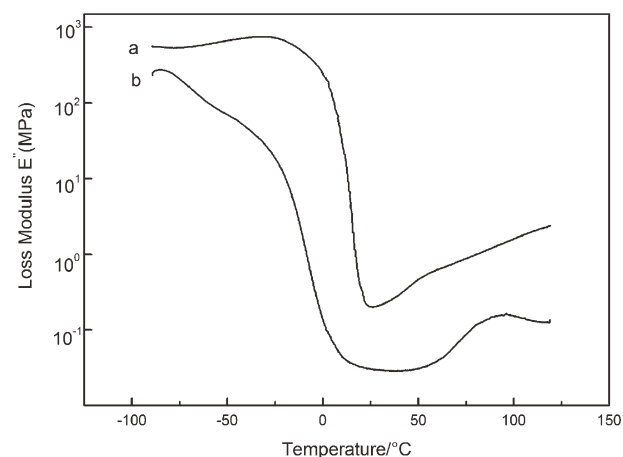


Figure 3 Loss modulus for PVA hydrogel (a) and IPN hydrogel (b) samples.

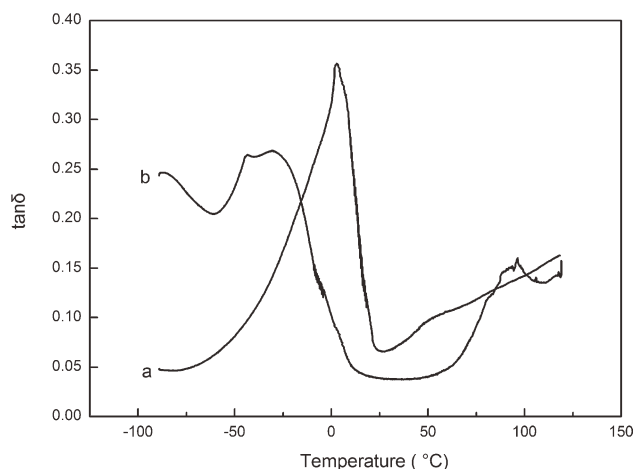


Figure 4 $\tan \delta$ value for PVA hydrogel (a) and IPN hydrogel (b) samples.

ascribed to the loss of the crystalline phase of the PVA component.

Differential scanning calorimetry (DSC)

The DSC thermograms for PVA and IPN hydrogels are shown in Figure 5. The sharp peak at 230°C represents the melting of crystallized PVA. The blend structure of IPN hydrogel includes amorphous PVP and part of the crystalline PVA; it shows a melting peak at about 222°C . The crystallinity (X_c) can be calculated according to a formula $X_c = \Delta H / \Delta H_c$,¹⁵ where ΔH is the heat required for melting a sample determined by integrating the area under the melting peak over the range 180 – 240°C , ΔH_c is the heat required for melting a 100% crystalline PVA sample (here $\Delta H_c = 138.6 \text{ J/g}$).¹⁶ The calculated crystallinity (X_c) of PVA hydrogel and IPN hydrogel is 65.3 and 26.3%, respectively. The structure of IPN obviously

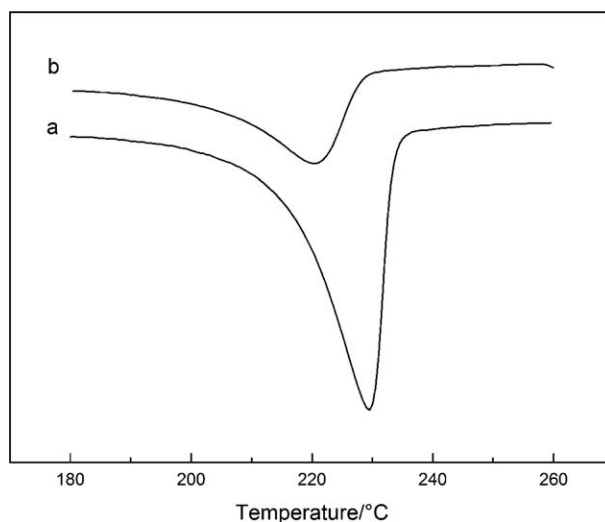


Figure 5 DSC curves of PVA hydrogel (a) and IPN hydrogel (b).

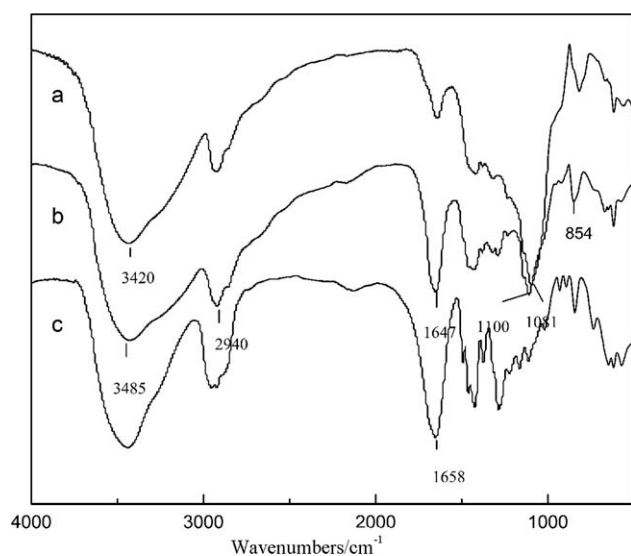


Figure 6 IR spectra of PVA (a), IPN (b), and PVP (c).

affected the crystallinity of hydrogel. It is mainly because that chain of PVP macromolecules separated PVA macromolecules, and inhibited the process of its crystallization. The hydrogen bonding between OH and C=O groups as polar groups had a large space hindering function on the movement of chain segment. Thus, the crystallinity was increased by preventing chain segment diffusing and arraying in crystal zone. The addition of PVP into PVA has a definite effect on the crystallinity of PVA in the blends over the whole composition range. This behavior can be explained by the higher viscosity of PVP blended in the melting state, which makes crystallization more difficult.

IR spectra

The IR spectra of pure PVA, pure PVP, and IPN hydrogel are shown in Figure 6. The broad band appeared at 3485 cm^{-1} in the spectrum (b) clearly marks the presence of hydrogen bonding and hydrophilic nature of IPN hydrogel.¹⁷ It also shows the presence of OH groups at 3420 cm^{-1} and C=O groups at 1658 cm^{-1} in spectrum (a) and spectrum (c). In addition, the peak at 1647 cm^{-1} shows the presence of CH₂ groups. The peak at 1081 cm^{-1} in spectrum (a) is attributed to the absorption of crystalline structure of PVA, which is attenuated sharply in IPN hydrogel. This is mainly due to the IPN structure impeding the crystallization of PVA to some extent. The pyrrolidone rings in PVP contain a proton accepting carbonyl moiety, while there are large amount of hydroxyl groups in PVA chains as side groups. Therefore, hydrogen bonding interaction may happen between the two chemical moieties after PVA and PVP being blended,^{18,19} which can affect the properties of the IPN hydrogel.

XPS analysis

As can be seen from the XPS spectra in Figure 7, the PVA hydrogel mainly shows C and O elements (a), while a new peak at 399.6 eV corresponding to N element appears in the IPN hydrogel (b). The binding energy of C1s and O1s of PVA is 284.7 and 532.1 eV , respectively. With the addition of PVP, the IPN hydrogel of PVA/PVP has obvious peak shift for C1s (285.2 eV) and O1s (531.3 eV). Further analysis for C1s and O1s peaks shown in Figure 8 exhibits that the C1s spectrum of IPN hydrogel can be divided into three main peaks with binding energy of 284.7 , 285.7 , and 287.4 eV , corresponding to the carbon atoms of saturated hydrocarbons (C–C), carbon atoms with a single bond to oxygen (C–O), and carbonyl group (C=O), respectively. The O1s spectrum of IPN shows that the contribution of O1s includes OH group of PVA and C=O group of PVP. The XPS

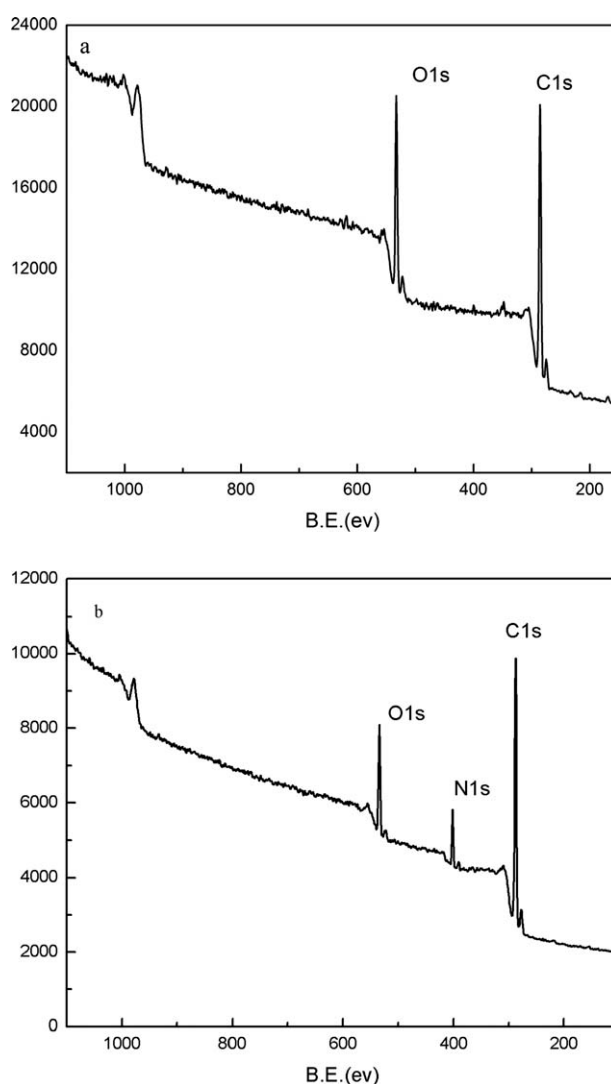


Figure 7 XPS spectra of PVA (a) and IPN hydrogel (b).

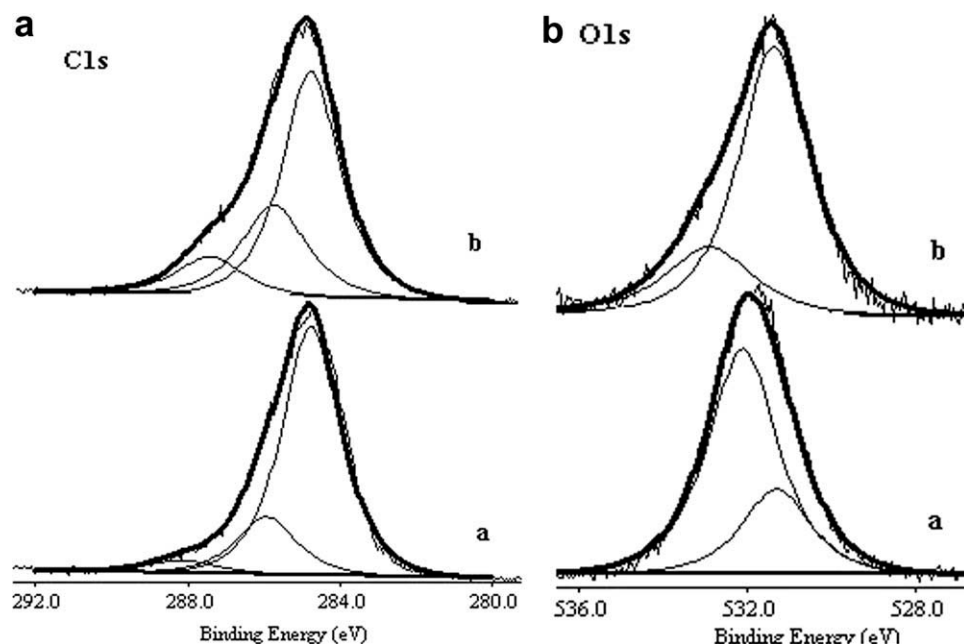


Figure 8 XPS spectra of the C1s and O1s peak: (a) PVA hydrogel and (b) IPN hydrogel.

analysis suggests that PVA and PVP are well miscible in the IPN hydrogel.

Scanning electron micrograph

The SEM images in Figure 9 show that the dried IPN hydrogel has three-dimensional porous structure and the pores are well interconnected, which endows the hydrogel with excellent water capacity. No obvious phase separation can be seen between PVA and PVP. This means PVP and PVA have good compatibility. In addition, the IPN hydrogel with high water content has a microporous structure [Fig. 9(b)] similar to that of natural cartilage tissues. The porous structure of IPN hydrogel is favorable for the attachment of cells and the exchange of nutritious substances. If loaded, water in the pores can easily influx or efflux and act as a lubricant in wear.

Mechanical properties

Mechanical properties such as tensile strength, compressive strength, and elongation at break are important for an artificial cartilage substitute. After the IPN hydrogel swelled sufficiently in deionized water at 37°C for five days, its tensile strength, compressive strength, and elongation at break are listed in Table I. It can be seen that all the values of IPN hydrogel are higher than those of PVA hydrogel. As we know, the mechanical strength of PVA hydrogel and IPN hydrogel will be affected by the crystallinity of PVA component. If only considering the crystallinity, PVA should have higher mechanical

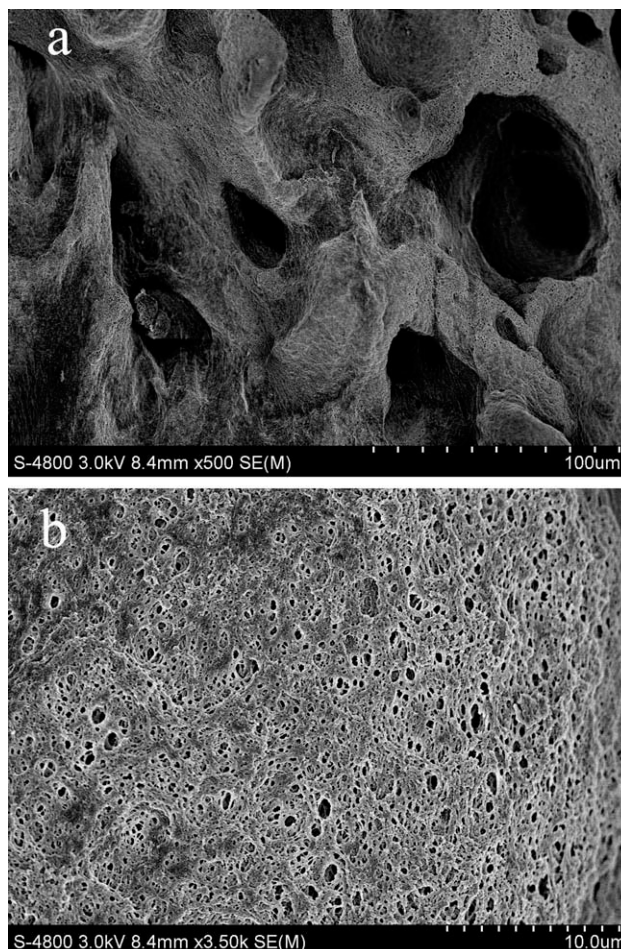


Figure 9 SEM images of dried IPN hydrogel: (a) $\times 500$; (b) $\times 3500$.

TABLE I
The Mechanical Properties of PVA and IPN Hydrogels

Hydrogel	Compressive strength (MPa)	Tensile strength (MPa)	Elongation (%)	Water content (%)
PVA	3.17 ± 0.23	1.23 ± 0.05	587 ± 46	65 ± 3
IPN	4.18 ± 0.16	4.13 ± 0.22	653 ± 40	68 ± 5

strength than IPN hydrogel, because PVA has a strong binding force due to the interaction of the pendant hydroxyl groups. After several freeze-thawing cycles, PVA hydrogel will form small crystal network at the crosslinking sites. The hydrogen bonds between PVA molecule chains can provide a high tensile strength. With the addition of PVP, the PVA network and molecule, regular arrangement will be partly destroyed, causing the decrease of hydrogen bonding density and the crystallinity, which may result in the decline of tensile strength. However, when crystallizable PVA blends with PVP, they can form well miscible IPN structure on a molecular level over the whole composition range and form intermolecular hydrogen bonds between them, although the intramolecular hydrogen bonds of PVA are partly broken. In addition, the two polymers reduce the average intermolecular distance and molecular motion of each component when mixed together.¹⁹ Thus, the IPN hydrogel obtains better mechanical performance. When mechanically loaded, the IPN structure can carry on more deformation, so the elongation at break of the IPN hydrogel is improved significantly. Compared with the tensile strength (>4 MPa) and other mechanical properties of human cartilage,²⁰ the IPN hydrogel has good performance on stretch and compression and may be used as a promising material for artificial cartilage substitute and orthopedics.

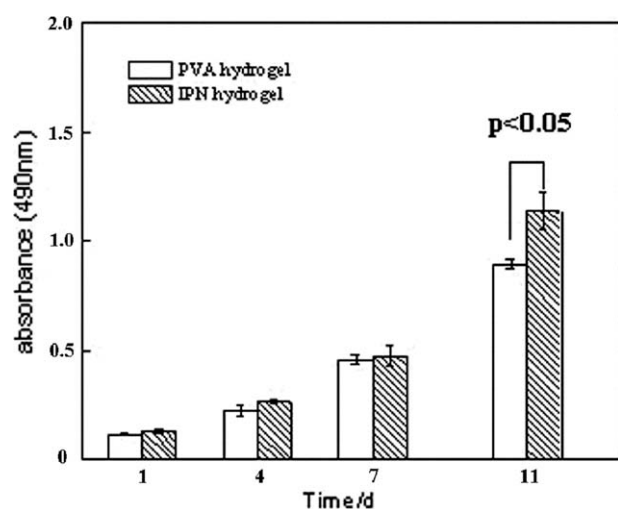


Figure 10 MSCs proliferation on hydrogels at different culture time, Error bars represent means \pm SD for $n = 3$.

Cell culture *in vitro*

Figure 10 shows the proliferation of MSCs cultured with IPN hydrogel and PVA hydrogel as contrast at 1, 4, 7, and 11 day(s). For a period of 11 days, the cell number continuously increases with the culture time on both tested groups. At day 11, the cell number of MSCs increases dramatically in both groups and the statistical analysis indicates that the number of cells seeded on IPN hydrogel is much higher than on PVA hydrogel ($P < 0.05$). The cell proliferation trend demonstrates that the addition of PVP has a positive influence on the cell growth. The result indicates that the IPN hydrogel has better cytocompatibility than PVA hydrogel.

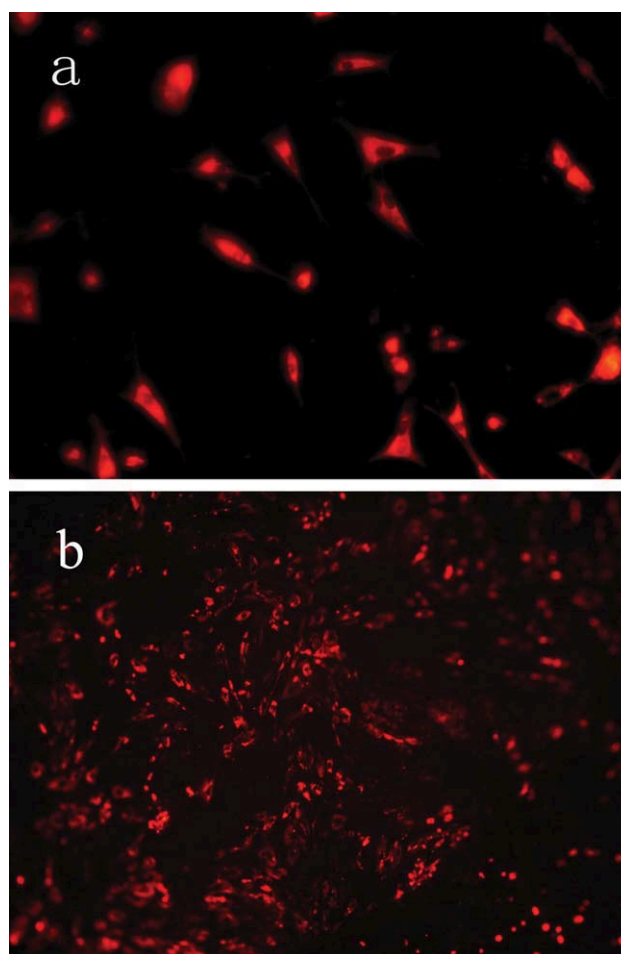


Figure 11 Images of MSCs by DiI stain for day 3 (a) and day 7 (b): (a) $\times 200$; (b) $\times 100$. [Color figure can be viewed in the online issue, which is available at [wileyonlinelibrary.com](http://www.interscience.wiley.com).]

MSCs were cultured with the IPN hydrogel for three and seven days and the cytotoxicity was evaluated through the observation of fluorescence microscope. It can be seen from Figure 11 that at day 3 in culture, the live cells adhere to and grow on the IPN hydrogel surface, exhibiting normal and healthy spindle-like morphology. At day 7, the number of MSCs increases with the incubation time and large amount of cells proliferate and aggregate, a confluent layer of cells appear on the hydrogel surface. The result indicates that the IPN hydrogel has no negative cellular response.

CONCLUSION

Compared with PVA hydrogel, the crystallization behavior, glass transition process, bond structure, and mechanical strength of PVA/PVP interpenetrating network (IPN) hydrogel have changed significantly. The IPN hydrogel has good performance on stretch and compression, high water content and microporous structure similar to natural cartilage. The liquid in the pores can easily influx and efflux, acting as a lubricant. Cell culture shows that the IPN hydrogel has good cytocompatibility. The results show that the IPN hydrogel can meet the basic requirement for biomaterial and can be used for further *in vivo* experiment.

References

1. Seal, B. L.; Otero, T. C.; Panitch, A. *Mater Sci Eng* 2001, 34, 147.
2. Cascone, M. G.; Sim, B.; Downes, S. *Biomaterials* 1995, 16, 569.
3. Pan, Y.; Xiong, D. *Wear* 2009, 266, 699.
4. Kobayashi, M.; Chang, Y.-S.; Oka, M. *Biomaterials* 2005, 26, 3243.
5. Thomas, J.; Lowman, A.; Marcolongo, M. *J Biomed Mater Res A* 2003, 67, 1329.
6. Seabra, A. B.; de Oliveira, M. G. *Biomaterials* 2004, 25, 3773.
7. Mei, G.; Yi, Z.; Qin, Z.; Li, Z.; Yubao, L. *Funct Mater* 2009, 3, 439.
8. Martens, P.; Anseth, K. S. *Polymer* 2000, 41, 7715.
9. Kim, S. J.; Park, S. J.; Kim, Y.; Chung, T. D.; Kim, H. C.; Kim, S. I. *J Appl Polym Sci* 2003, 90, 881.
10. Sperling, L. H. *Interpenetrating Polymer Networks and Related Materials*; Plenum Press: New York, 1981.
11. Cowie, J. M. G. In *Encyclopedia of Polymer Science and Engineering*, 2nd edn.; Mark, H. F., Bikales, N. M., Overberger, C. G., Menges, G., Kroschwitz, J. I., Eds.; Wiley: New York, 1988.
12. Cassu, S. N.; Felisberti, M. I. *Polymer* 1997, 38, 3907.
13. Zou, Q.; Li, Y. B.; Zhang, L.; Zuo, Y.; Li, J. F.; Li, X. Y. *J Biomed Mater Res* 2008, 90B, 156.
14. Julien, M.; Khairoun, I.; LeGeros, R. Z.; Delplace, S.; Pilet, P.; Weiss, P.; Daculsi, G.; Bouler, J. M. *Biomaterials* 2007, 28, 956.
15. Peppas, N. A.; Hansen, P. J. *J Appl Polym Sci* 1982, 27, 4787.
16. Peppas, N. A.; Merrill, E. W. *J Appl Polym Sci* 1976, 20, 1457.
17. Mishra, S.; Bajpai, R.; Katare, R.; Bajpai, A. K. *J Mater Sci: Mater Med* 2006, 17, 1305.
18. Feng, H.; Feng, Z.; Shen, L. *Polymer* 1993, 34, 2516.
19. Zhang, X.; Takegoshi, K.; Hikichi, K. *Polymer* 1992, 33, 712.
20. Abdel-Rahman, E. M.; Hefzy, M. S. *Med Eng Phys* 1998, 20, 276.